J. Fluid Mech. (1965), *vol.* 23, *part* 3, *pp.* 439–458
Printed in Great Britain

The base-flow and near-wake problem at very low Reynolds numbers

Part 2. The Oseen approximation

By H. VIVIAND AND S. A. BERGER
University of California, Berkeley

(Received 2 February 1965 and in revised form 18 May 1965)

The influence of inertia terms in the equations of motion on the properties of the base-flow and near-wake flow at very low Reynolds numbers is investigated by using Oseen's approximation and by comparing with the results obtained in Part 1 for Stokes flow. The general solutions of Oseen's equations of motion are derived for two-dimensional and axisymmetric flows in the half-space $x > 0$, for an arbitrarily given velocity field in the plane $x = 0$. Numerical examples are given for two-dimensional flow and compared with Stokes-flow examples.

1. Introduction

In Part 1 a study was made of the base-flow problem for low Reynolds numbers, the basic assumption being that the non-linear convection terms were negligible and could be dropped from the equation of motion. The basic equations could then be solved with arbitrary boundary conditions for both plane and axisymmetric flows.

In this part, the Oseen approximate equations of motion are considered. In this approximation the convection is assumed to take place with some constant velocity rather than the actual local velocity. In its original form, Oseen's theory takes this convection velocity equal to the free-stream velocity so that the Navier–Stokes equations are represented with great accuracy in regions of the flow field far from any solid surface. Following Lewis & Carrier (1949), we use a convection velocity equal to cU, where the constant c lies in the range $0 < c < 1$ and is to be chosen so as to obtain a more accurate representation of the convection velocity over the entire flow field.

The Oseen equations, like the Stokes equations, are valid approximations at low Reynolds numbers,† and in contrast to the Stokes equations are uniformly valid at large distances from solid bodies. However, in the context of the base-flow problem, it is not clear whether or not they represent an improvement over the Stokes equations; this will depend on the particular conditions considered. In a general way if $\delta \gg 1$, where $\delta = \delta_1/a_1$ is the ratio of initial boundary-layer thickness to base height or radius (figure 1), then the Oseen approximation is likely to be more accurate; on the other hand, if $\delta \approx 1$, the base-flow region takes

† We exclude from this discussion the case where the Oseen linearization is based on a small perturbation type analysis, independent of the magnitude of the Reynolds number.

on more importance and the inclusion of linearized inertia terms may be a worse approximation in this region than completely neglecting them.

Therefore the Oseen approximation is not put forward as a specific improvement upon the Stokes approximation, but rather as a means of evaluating the effects of increasing Reynolds number; the results being given only qualitative value, we shall allow the Reynolds number to take on values larger than the maximum ones permitted in Stokes flow.

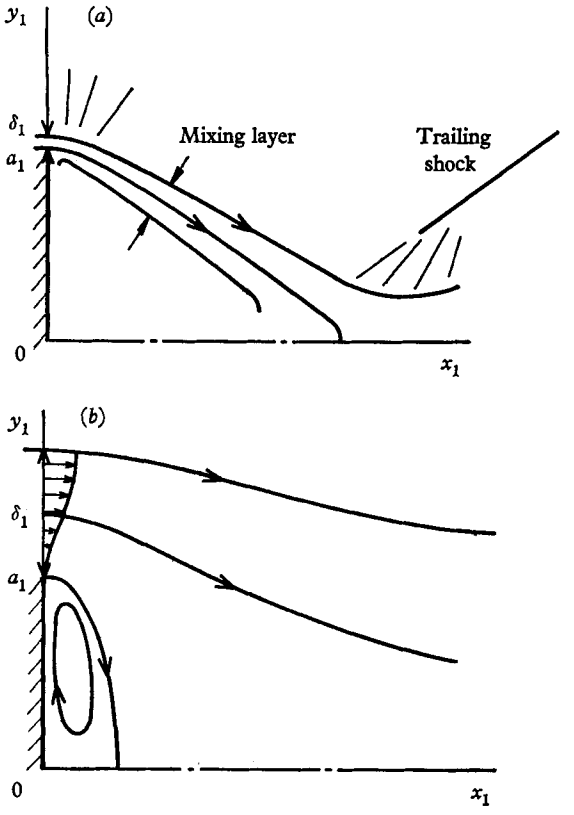

FIGURE 1. Sketch of base flow: (*a*) high-Reynolds-number, supersonic flow; (*b*) low-Reynolds-number flow.

2. The basic equations

Setting $u = c$ and $v = 0$ in equations (2.2) of Part 1, and introducing

$$R = \tfrac{1}{2}cR_{a_1}, \tag{2.1}$$

we obtain the Oseen form of the momentum equations

$$2R\frac{\partial}{\partial x}\left(\frac{p}{c}+u\right) = -y^{-j}\frac{\partial}{\partial y}(y^j\Omega), \tag{2.2a}$$

$$2R\frac{\partial}{\partial y}\left(\frac{p}{c}+u\right) + 2R\Omega = \frac{\partial\Omega}{\partial x}. \tag{2.2b}$$

The corresponding vorticity equation is given by

$$2R\frac{\partial\Omega}{\partial x} = \frac{\partial^2\Omega}{\partial x^2} + \frac{\partial^2\Omega}{\partial y^2} + j\left(\frac{1}{y}\frac{\partial\Omega}{\partial y} - \frac{\Omega}{y^2}\right). \tag{2.3}$$

The method of solution is as follows: the vorticity equation (2.3) is solved first, assuming that $\Omega(0, y) = \Omega_i(y)$ is given. The stream function is then obtained from equation (2·6) of Part 1 if $\psi(0, y) = \psi_i(y)$ is known, and the pressure results from equations (2·2). Once this solution has been obtained, one can easily deduce the solution which corresponds to given $v(0, y) = v_i(y)$ instead of $\Omega_i(y)$, and to given $\psi_i(y)$.

3. Two-dimensional Oseen flow

3.1. *The vorticity*

With $j = 0$, equation (2.3) becomes

$$2R\frac{\partial\Omega}{\partial x} = \frac{\partial^2\Omega}{\partial x^2} + \frac{\partial^2\Omega}{\partial y^2}, \tag{3.1}$$

and is to be solved in the half-plane $x > 0$, with the boundary condition

$$\Omega(0, y) = \Omega_i(y). \tag{3.2}$$

The method of separation of variables yields the following solution†

$$\Omega = \exp(-Kx)(A\cos\lambda y + B\sin\lambda y),$$

where

$$K = \sqrt{(R^2+\lambda^2)} - R. \tag{3.3}$$

Equation (3.1) being linear, a more general solution can be constructed, of the form

$$\Omega(x, y) = \int_0^\infty \exp(-Kx)[A(\lambda)\cos\lambda y + B(\lambda)\sin\lambda y]\,d\lambda, \tag{3.4}$$

where $A(\lambda)$ and $B(\lambda)$ are arbitrary functions with the only restriction that the integral shall exist.

Equation (3.4) will represent the solution if condition (3.2) can be satisfied, namely

$$\Omega_i(y) = \int_0^\infty [A(\lambda)\cos\lambda y + B(\lambda)\sin\lambda y]\,d\lambda. \tag{3.5}$$

Separating each side of equation (3.5) into even and odd components in y, we obtain

$$\tfrac{1}{2}[\Omega_i(y) + \Omega_i(-y)] = \int_0^\infty A(\lambda)\cos\lambda y\,d\lambda, \tag{3.6a}$$

$$\tfrac{1}{2}[\Omega_i(y) - \Omega_i(-y)] = \int_0^\infty B(\lambda)\sin\lambda y\,d\lambda. \tag{3.6b}$$

Fourier reciprocity formulae then give (Courant & Hilbert 1962, vol. I, p. 80)

$$A(\lambda) = \frac{1}{\pi}\int_0^\infty [\Omega_i(y) + \Omega_i(-y)]\cos\lambda y\,dy, \tag{3.7a}$$

$$B(\lambda) = \frac{1}{\pi}\int_0^\infty [\Omega_i(y) - \Omega_i(-y)]\sin\lambda y\,dy, \tag{3.7b}$$

† Another solution is $\exp(K'x)(A\cos\lambda y + B\sin\lambda y)$, where $K' = \sqrt{(R^2+\lambda^2)} + R$ but is unacceptable since it goes to infinity with x.

and, inversely, equations (3.6) and (3.5) follow from equations (3.7); in particular if $A(\lambda)$ and $B(\lambda)$, as defined by equations (3.7), exist, then equation (3.4) has a meaning and gives the solution. In what follows, we assume that $\Omega_i(y) \to 0$ as $|y| \to \infty$ fast enough for $A(\lambda)$ and $B(\lambda)$ to exist.

In the particular case of symmetric flow, we have $\Omega_i(-y) = -\Omega_i(y)$ and equations (3.7) become

$$A(\lambda) = 0, \tag{3.8a}$$

$$B(\lambda) = \frac{2}{\pi}\int_0^\infty \Omega_i(y) \sin \lambda y \, dy. \tag{3.8b}$$

3.2. *The stream function*

In two-dimensional flow, equation (2.6) of Part 1 is Poisson's equation

$$\nabla^2 \psi = -\Omega(x, y),$$

where Ω is now given by equation (3.4); we add the boundary condition

$$\psi(0, y) = \psi_i(y).$$

Let us decompose ψ into a potential and a rotational component

$$\psi = \psi_P + \psi_R, \tag{3.9}$$

such that

$$\nabla^2 \psi_P = 0, \qquad \psi_P(0, y) = \psi_i(y),$$

$$\nabla^2 \psi_R = -\Omega(x, y), \quad \psi_R(0, y) = 0.$$

ψ_P is obtained immediately by means of Poisson's integral for a half-plane (Courant & Hilbert 1962, vol. II, p. 268)

$$\psi_P = \frac{1}{\pi}\int_{-\infty}^{\infty} \frac{x}{x^2 + (\eta - y)^2} \psi_i(\eta) \, d\eta. \tag{3.10}$$

To solve for ψ_R, we follow the technique of separation of variables used for Ω; the calculations are shown in Appendix I, and the result is

$$\psi_R = \frac{1}{2R}\int_0^\infty [\sqrt{(R^2 + \lambda^2)} + R][\exp(-Kx) - \exp(-\lambda x)] \times [A(\lambda)\cos \lambda y + B(\lambda) \sin \lambda y] \frac{1}{\lambda^2} d\lambda. \tag{3.11}$$

3.3. *The velocity field*

According to equation (3.9), we can write

$$u = u_P + u_R, \quad v = v_P + v_R,$$

with

$$u_P = \partial \psi_P / \partial y, \quad v_P = -\partial \psi_P / \partial x,$$

$$u_R = \partial \psi_R / \partial y, \quad v_R = -\partial \psi_R / \partial x.$$

The general expressions for u and v are then easily obtained through equations (3.10) and (3.11). The only difficulty concerns the calculation of v_P at $x = 0$, since this quantity cannot be obtained directly from equation (3.10).

Let us calculate $v_P(x, y)$ in a different way, using

$$\frac{\partial v_P}{\partial x} = \frac{\partial u_P}{\partial y} \quad (\text{since } \nabla^2 \psi_P = 0)$$

and

$$\nabla^2 u_P = 0, \quad u_P(0, y) = u_i(y).$$

Following the method of § 3.1 in the particular case of $R = 0$, and restricting the calculations to the case of symmetric flow,† we find

$$1 - u_P(x, y) = \int_0^\infty \exp(-\lambda x) \cos \lambda y \frac{C(\lambda)}{\lambda} d\lambda, \tag{3.12}$$

where

$$\frac{C(\lambda)}{\lambda} = \frac{2}{\pi} \int_0^\infty [1 - u_i(y)] \cos \lambda y \, dy.$$

After an integration by parts we obtain

$$C(\lambda) = \frac{2}{\pi} \int_0^\infty \frac{du_i(y)}{dy} \sin \lambda y \, dy. \tag{3.13}$$

Therefore

$$\frac{\partial v_P}{\partial x} = \frac{\partial u_P}{\partial y} = \int_0^\infty \exp(-\lambda x) \sin \lambda y \, C(\lambda) \, d\lambda,$$

and

$$v_P(x, y) = -\int_0^\infty \exp(-\lambda x) \sin \lambda y \frac{C(\lambda)}{\lambda} d\lambda. \tag{3.14}$$

From equations (3.11) and (3.14) we now deduce $v_i(y)$ for symmetric flows

$$v_i(y) = -\int_0^\infty \left[C(\lambda) + \frac{\sqrt{(R^2 + \lambda^2)} + R - \lambda}{2R} B(\lambda) \right] \frac{1}{\lambda} \sin \lambda y \, d\lambda. \tag{3.15}$$

As far as the numerical calculation of u_P is concerned, equation (3.12) may be replaced with advantage by Poisson's integral

$$u_P(x, y) = \frac{1}{\pi} \int_{-\infty}^\infty \frac{x}{x^2 + (\eta - y)^2} u_i(\eta) \, d\eta. \tag{3.16}$$

Using equations (3.11) and (3.16), the velocity on the x-axis, for symmetric flows, is found to be

$$u_0(x) = u_P(x, 0) + u_R(x, 0), \tag{3.17a}$$

where

$$u_P(x, 0) = \frac{2}{\pi} \int_0^\infty \frac{x}{x^2 + \eta^2} u_i(\eta) \, d\eta, \tag{3.17b}$$

$$u_R(x, 0) = \frac{1}{2R} \int_0^\infty [\sqrt{(R^2 + \lambda^2)} + R] \exp(-Kx) - \exp(-\lambda x) \frac{B(\lambda)}{\lambda} d\lambda. \tag{3.17c}$$

3.4. *The pressure field*

Equation (2.2a), with $j = 0$, together with equation (3.4), results in

$$\frac{p - p_\infty}{c} + u - 1 = \frac{1}{2R} \int_0^\infty [\sqrt{(R^2 + \lambda^2)} + R] \exp(-Kx) \times [B(\lambda) \cos \lambda y - A(\lambda) \sin \lambda y] (1/\lambda) \, d\lambda. \tag{3.18}$$

† The extension to asymmetric flows is obvious and is not given here to simplify the equations.

Equation (2.2b) is then automatically satisfied, as one would expect, since equation (2.3), which has been used to solve for Ω, is a consequence of the two equations (2.2).

On the x-axis, we find

$$\frac{p_0(x)-p_\infty}{c} = 1-u_0(x)+\frac{1}{2R}\int_0^\infty [\sqrt{(R^2+\lambda^2)}+R]\exp(-Kx)\frac{B(\lambda)}{\lambda}d\lambda. \quad (3.19)$$

The pressure at $x = 0$, in the case of symmetric flow, is

$$\frac{p_i(y)-p_\infty}{c} = 1-u_i(y)+\frac{1}{2R}\int_0^\infty [\sqrt{(R^2+\lambda^2)}+R]\cos\lambda y\frac{B(\lambda)}{\lambda}d\lambda. \quad (3.20)$$

3.5. *Solution in terms of $v_i(y)$*

Here also we restrict the calculations to symmetric flow. We assume now that $v_i(y)$ is given as a boundary condition instead of $\Omega_i(y)$ so that $B(\lambda)$ is unknown. Let $D(\lambda)$ be the inverse Fourier sine transform of $v_i(y)$

$$D(\lambda) = \frac{2}{\pi}\int_0^\infty \sin\lambda y\, v_i(y)\,dy, \quad (3.21)$$

so that

$$v_i(y) = \int_0^\infty \sin\lambda y D(\lambda)\,d\lambda, \quad (3.22)$$

since $v_i(y)$ is assumed to be an odd function of y.

Comparing equations (3.22) and (3.15), we see that

$$D(\lambda) = -\frac{C(\lambda)}{\lambda}-\frac{1}{2R}[\sqrt{(R^2+\lambda^2)}+R-\lambda]\frac{B(\lambda)}{\lambda}.$$

Hence

$$B(\lambda) = -2R\frac{\lambda D(\lambda)+C(\lambda)}{\sqrt{(R^2+\lambda^2)}+R-\lambda} \quad (3.23a)$$

$$= -[\sqrt{(R^2+\lambda^2)}+\lambda-R]\left[D(\lambda)+\frac{C(\lambda)}{\lambda}\right]. \quad (3.23b)$$

When $B(\lambda)$ is determined, the solution presented in §§ 3.1 to 3.4 applies.

4. Axisymmetric Oseen flow

The calculations concerning axisymmetric flow follow very closely those of § 3 for two-dimensional flow, and the results show a striking similarity; the main difference lies in the use of Fourier–Bessel integrals instead of Fourier sine or cosine transforms.

4.1. *The vorticity*

With $j = 1$, equation (2.3) becomes

$$2R\frac{\partial\Omega}{\partial x} = \frac{\partial^2\Omega}{\partial x^2}+\frac{\partial^2\Omega}{\partial y^2}+\frac{1}{y}\frac{\partial\Omega}{\partial y}-\frac{\Omega}{y^2}, \quad (4.1)$$

and is to be solved for $x \geqslant 0$, $y \geqslant 0$, with the boundary conditions

$$\Omega(0,y) = \Omega_i(y), \quad (4.2a)$$

$$\Omega(x,0) = 0. \quad (4.2b)$$

By the method of separation of variables, we find the following solution to equation (4.1)

$$\Omega(x,y) = \int_0^\infty \exp(-Kx)\, J_1(\lambda y)\, \lambda A(\lambda)\, d\lambda, \tag{4.3}$$

where $K = \sqrt{(R^2+\lambda^2)} - R$, and where $J_1(z)$ is the Bessel function of order 1. Condition (4.2*b*) is then satisfied and condition (4.2*a*) gives

$$\Omega_i(y) = \int_0^\infty J_1(\lambda y)\, \lambda A(\lambda)\, d\lambda. \tag{4.4}$$

According to the Fourier–Bessel double integral formula (Bowman 1958, pp. 113–14), we have

$$\Omega_i(y) = \int_0^\infty J_1(\lambda y)\, \lambda \int_0^\infty \Omega_i(t)\, J_1(\lambda t)\, t\, dt\, d\lambda,$$

so that condition (4.4) will be satisfied by taking

$$A(\lambda) = \int_0^\infty \Omega_i(t)\, J_1(\lambda t)\, t\, dt. \tag{4.5}$$

We have assumed all the preceding integrals to exist; a sufficient condition for this to be true is that (Bowman 1958)

$$\Omega_i(t)\, t^{\frac{3}{2}} \to 0 \quad \text{as} \quad t \to \infty.$$

4.2. *The stream function*

Equation (2.6) of Part 1, with $j = 1$, becomes

$$D^2\psi = -y\Omega(x,y), \tag{4.6}$$

where Ω is given by equation (4.3); equation (4.6) is to be solved for $x \geqslant 0, y \geqslant 0$, with the boundary conditions

$$\psi(0,y) = \psi_i(y), \tag{4.7a}$$

$$\psi(x,0) = 0. \tag{4.7b}$$

Let

$$\psi = \psi_P + \psi_R, \tag{4.8}$$

where

$$D^2\psi_P = 0, \qquad \psi_P(0,y) = \psi_i(y), \qquad \psi_P(x,0) = 0,$$

$$D^2\psi_R = -y\Omega(x,y), \qquad \psi_R(0,y) = 0, \qquad \psi_R(x,0) = 0.$$

The solution for ψ_P has already been given in connexion with Stokes flow (see equation (5.3) and Appendix I of Part 1):

$$\psi_P(x,y) = \frac{3}{\pi} y^2 \int_{\eta=0}^\infty \int_{\theta=0}^\pi \frac{x \sin^2\theta\, \eta \psi_i(\eta)}{[x^2+y^2+\eta^2-2y\eta\cos\theta]^{\frac{5}{2}}}\, d\theta\, d\eta. \tag{4.9}$$

The calculation of ψ_R is shown in Appendix I; we find

$$\psi_R = \frac{1}{2R} y \int_0^\infty [\sqrt{(R^2+\lambda^2)} + R][\exp(-Kx) - \exp(-\lambda x)]\, J_1(\lambda y) \frac{A(\lambda)}{\lambda}\, d\lambda. \tag{4.10}$$

4.3. *The velocity field*

Following the decomposition (4.8), we let

$$u = u_P + u_R, \qquad v = v_P + v_R,$$

with

$$u_P = y^{-1}(\partial\psi_P/\partial y), \quad v_P = -y^{-1}(\partial\psi_P/\partial x),$$

$$u_R = y^{-1}(\partial\psi_R/\partial y), \quad v_R = -y^{-1}(\partial\psi_R/\partial x),$$

so that u and v are easily obtained from equations (4.9) and (4.10), with the exception of $v_P(0, y)$.

As in § 2.3, let us calculate $v_P(x, y)$ in a different way. From $D^2\psi_P = 0$, we deduce

$$\left[\frac{\partial^2}{\partial x^2} + \frac{\partial^2}{\partial y^2} + \frac{1}{y}\frac{\partial}{\partial y} - \frac{1}{y^2}\right]\frac{\partial u_P}{\partial y} = 0. \tag{4.11}$$

We also have

$$\frac{\partial u_P}{\partial y}(0, y) = \frac{du_i(y)}{dy}.$$

Note that equation (4.11) is of the form of equation (4.1) with $R = 0$; therefore, following the method of § 4.1, we find

$$\frac{\partial u_P}{\partial y} = \int_0^\infty \exp(-\lambda x)\, J_1(\lambda y)\, \lambda C(\lambda)\, d\lambda,$$

where

$$C(\lambda) = \int_0^\infty \frac{du_i(t)}{dt}\, t J_1(\lambda t)\, dt. \tag{4.12}$$

Now using $\partial v_P/\partial x = \partial u_P/\partial y$, and after an integration with respect to x, we obtain

$$v_P(x, y) = -\int_0^\infty \exp(-\lambda x)\, J_1(\lambda y)\, C(\lambda)\, d\lambda. \tag{4.13}$$

We then use equations (4.10) and (4.13) to calculate $v(0, y) = v_i(y)$

$$v_i(y) = -\int_0^\infty \left[C(\lambda) + \frac{\sqrt{(R^2+\lambda^2)} + R - \lambda}{2R} A(\lambda)\right] J_1(\lambda y)\, d\lambda. \tag{4.14}$$

The velocity on the x-axis, $u_0(x)$, can be obtained as the limit, as $y \to 0$, of $2\psi/y^2$. Using equations (4.9) and (4.10), we find

$$u_0(x) = u_P(x, 0) + u_R(x, 0), \tag{4.15a}$$

with

$$u_P(x, 0) = 3x \int_0^\infty \frac{\eta\psi_i(\eta)}{(x^2+\eta^2)^{\frac{5}{2}}}\, d\eta, \tag{4.15b}$$

$$u_R(x, 0) = \frac{1}{2R}\int_0^\infty [\sqrt{(R^2+\lambda^2)} + R][\exp(-Kx) - \exp(-\lambda x)]\, A(\lambda)\, d\lambda. \tag{4.15c}$$

By successive integrations by parts, equation (4.15b) can be transformed into (using $\psi_i(0) = 0$)

$$u_P(x, 0) = x \int_0^\infty \frac{\eta u_i(\eta)}{(x^2+\eta^2)^{\frac{3}{2}}}\, d\eta, \tag{4.15d}$$

$$= x \int_0^\infty \frac{du_i/d\eta}{(x^2+\eta^2)^{\frac{1}{2}}}\, d\eta + u_i(0). \tag{4.15e}$$

4.4. *The pressure field*

Equation (2.2*a*), with $j = 1$, is easily integrated, and we find

$$\frac{p-p_\infty}{c}+u-1=\frac{1}{2R}\int_0^\infty [\sqrt{(R^2+\lambda^2)}+R]\exp(-Kx)\,J_0(\lambda y)\,A(\lambda)\,d\lambda, \quad (4.16)$$

where $J_0(z)$ is the Bessel function of zero order and the relation

$$J_1(z)+zJ_1'(z)=zJ_0(z)$$

has been used. Equation (2.2*b*) is then automatically satisfied.

4.5. *Solution in terms of* $v_i(y)$

Now we assume that $v_i(y)$ is given as a boundary condition, instead of $\Omega_i(y)$, so that $A(\lambda)$ is unknown. Applying the Fourier–Bessel double integral formula to v_i, we can write

$$v_i(y)=\int_0^\infty \lambda J_1(\lambda y)\,D(\lambda)\,d\lambda, \quad (4.17)$$

where

$$D(\lambda)=\int_0^\infty tJ_1(\lambda t)\,v_i(t)\,dt. \quad (4.18)$$

Comparing equation (4.17) with (4.14), we see that

$$\lambda D(\lambda)=-C(\lambda)-\frac{1}{2R}[\sqrt{(R^2+\lambda^2)}+R-\lambda]A(\lambda).$$

Hence

$$A(\lambda)=-2R\frac{\lambda D(\lambda)+C(\lambda)}{\sqrt{(R^2+\lambda^2)}+R-\lambda} \quad (4.19a)$$

$$=-[\sqrt{(R^2+\lambda^2)}+\lambda-R]\left[D(\lambda)+\frac{C(\lambda)}{\lambda}\right]. \quad (4.19b)$$

5. Numerical examples and discussion

5.1. *Generalities*

The main purpose for studying the Oseen solution to the base-flow problem being a qualitative evaluation of the inertia effects which were neglected in the Stokes solution, numerical examples have been carried out only for two-dimensional symmetric flows. The examples of Stokes flow presented in § 6 of Part 1 show that there is no remarkable difference between the two-dimensional and axisymmetric cases, and the results of §§ 3 and 4 of this Part show that this similarity persists in Oseen flow.

Conditions were furthermore restricted to the case $v_i(y) \equiv 0$, so that the required boundary condition, $v_i(y) = 0$ for $|y| < 1$, was satisfied in the simplest possible way. The initial velocity profile (x-component) was then chosen as

$$u_i(y)=\begin{cases}0 & (0\leqslant y\leqslant 1),\\ \left(\frac{y-1}{\delta}\right)^3\left\{10-15\frac{y-1}{\delta}+6\left(\frac{y-1}{\delta}\right)^2\right\} & (1\leqslant y\leqslant \delta+1),\\ 1 & (y\geqslant \delta+1),\end{cases} \quad (5.1)$$

$$u_i(-y)=u_i(y) \quad \text{(symmetric flow)}.$$

This profile has the property that du_i/dy and d^2u_i/dy^2 are everywhere continuous, in particular at $y = 1$ and $y = \delta + 1$; it will be shown in Appendix III that, as in Stokes flow, du_i/dy must be continuous if the pressure is to remain bounded. Equation (5.1) is represented in figure 2 (curve II) for $\delta = 1$; one sees that there is very little difference with the cosine profile (curve I) used in Stokes flow (§ 6 of Part 1) so that comparison with the examples of Stokes flow will be possible.

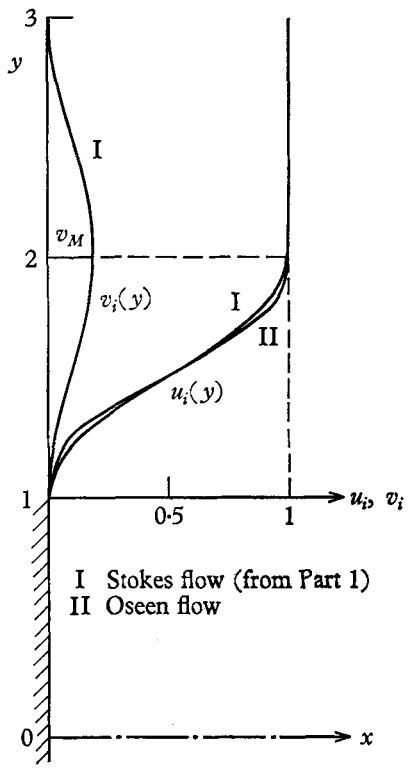

FIGURE 2. Velocity profiles at $x = 0$. $\delta = 1$.

In order to study the effects of Reynolds numbers, the initial boundary-layer thickness δ_1 was changed together with R_{L_1}, according to boundary-layer theory,† namely, $\delta_1 \sim L_1/\sqrt{R_{L_1}}$. For a particular solution to be determined, only δ and $R = \frac{1}{2}cR_{a_1}$ need to be given; we expect that an 'optimum' value for c, determined for instance by comparison with experimental results, would change with δ, very likely increasing with δ; but, since we do not have enough information about this, the value of c is assumed to remain constant, although not actually specified, as R_{L_1} and δ vary.

Taking $\delta_1/L_1 = \alpha/\sqrt{R_{L_1}}$ we find that

$$\delta = \delta_1/a_1 = \alpha\sqrt{\{L_1 c/(2a_1 R)\}}.$$

The calculations were carried out for

$$\delta = \sqrt{(3/R)},$$

† Even though R_{L_1} may be too small for this to be accurate.

corresponding to $\alpha^2 L_1 c/a_1 = 6$. To illustrate this discussion, let us take the following hypothetical values:

$$\alpha^2 = 10, \quad c = 0{\cdot}1, \quad L_1/a_1 = 6.$$

We can then find the values of Reynolds numbers for the values of δ used in the examples, and these are given in table 1.

The only quantities calculated are the velocity and pressure on the x-axis and the pressure at $x = 0$. The method of calculation is described in Appendix II.

δ	$R = 3/\delta^2$	$R_{a_1} = 20R$	$R_{L_1} = 120R$
0·6	8·33	166·66	1000
1·0	3·0	60·0	360
1·4	1·53	30·61	183·7
2·2	0·62	12·4	74·4

TABLE 1

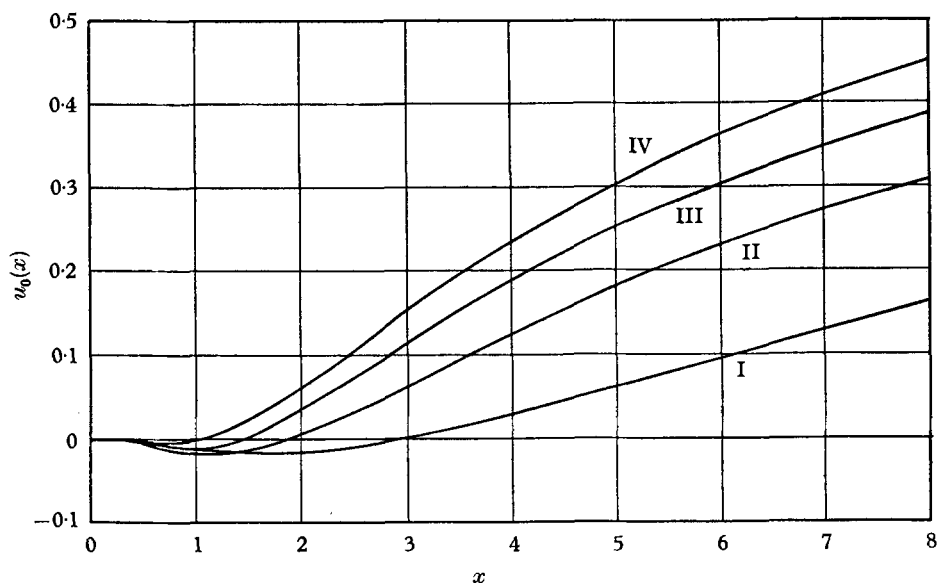

FIGURE 3. Velocity on x-axis for two-dimensional Oseen flow. $v_i \equiv 0$. Curve I, $\delta = 0{\cdot}6$, $R = 3/\delta^2 = 8{\cdot}33$; II, $\delta = 1{\cdot}0, R = 3{\cdot}0$; III, $\delta = 1{\cdot}4, R = 1{\cdot}53$; IV, $\delta = 2{\cdot}2, R = 0{\cdot}62$.

5.2. *Velocity on x-axis*

Figure 3 shows the velocity on the x-axis for various δ. We notice the existence of negative velocities indicating a recirculating flow region; this does not happen in Stokes flow when $v_i \equiv 0$ and therefore we can conclude that inertia effects alone are responsible for the existence of this recirculating zone. More precisely, we should compare curve A $\{u_0(x)\}$ of figure 7 of Part 1 with curve II of figure 3, corresponding respectively to $R = 0$ and $R = 3$, both for $\delta = 1$ and practically identical boundary conditions. The recirculating zone, which does not exist at $R = 0$, extends downstream over a distance equal to $1{\cdot}9a_1$ at $R = 3$, and is accompanied by a lower rate of increase of u_0 with x.

Curves I to IV (figure 3) show how the combined variations of R and δ affect $u_0(x)$; of particular interest is the position of the rear stagnation point, shown in figure 5 as a function of R. As $R \to 0$, the rear stagnation point moves upstream

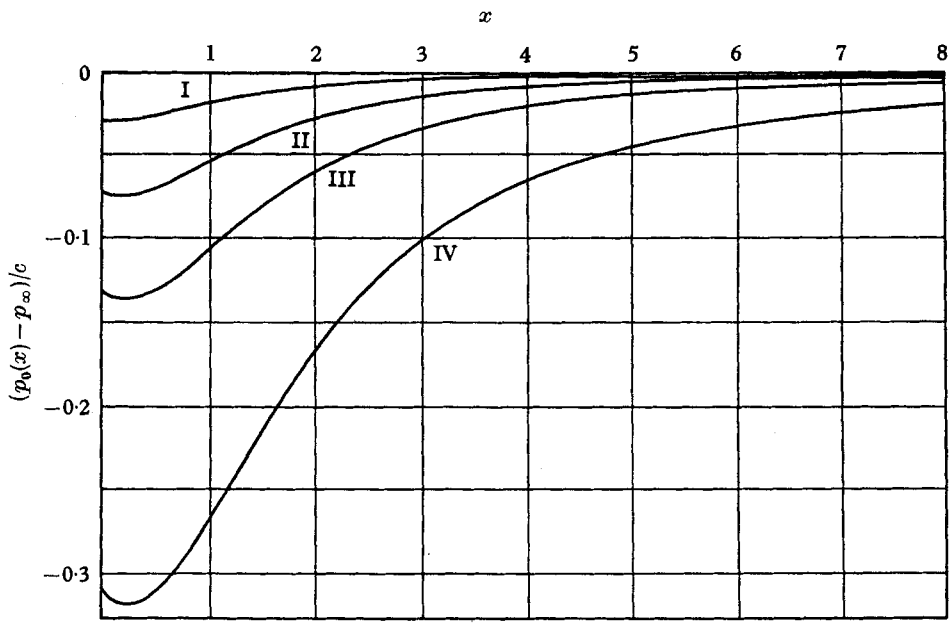

FIGURE 4. Pressure on x-axis for two-dimensional Oseen flow. $v_i \equiv 0$. Curve I, $\delta = 0{\cdot}6$, $R = 3/\delta^2 = 8{\cdot}33$; II, $\delta = 1{\cdot}0$, $R = 3{\cdot}0$; III, $\delta = 1{\cdot}4$, $R = 1{\cdot}53$; IV, $\delta = 2{\cdot}2$, $R = 0{\cdot}62$.

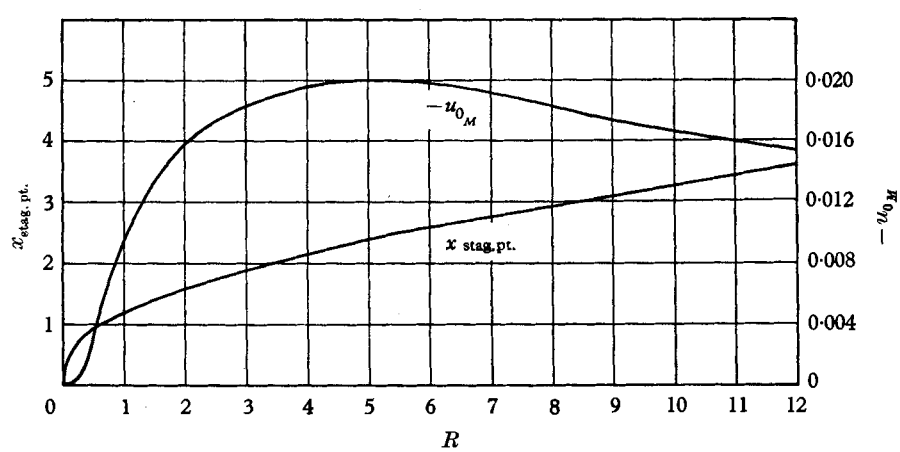

FIGURE 5. Position of rear stagnation point and maximum backflow velocity in two-dimensional Oseen flow. $v_i \equiv 0$, $\delta = \sqrt{(3/R)}$.

until it reaches the base for $R = 0$ (since $v_i \equiv 0$); we know that, in the case $v_i(y) \geqslant 0$, the limiting position would be slightly downstream of the base. As R increases the rear stagnation point moves continuously downstream; but we must, of course, restrict the results to relatively small values of R, and the fact

that the length of the separated flow region goes to infinity with R is of no significance here.

Also of interest is the maximum backflow velocity u_{0_M} shown in figure 5. $|u_{0_M}|$ goes through a maximum of 0·02 at $R \approx 5$ and then decreases as R increases;

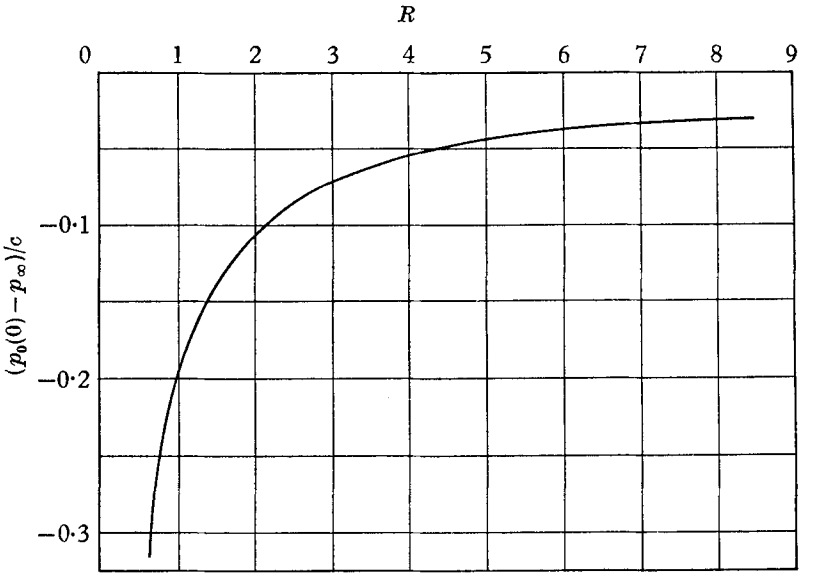

FIGURE 6. Pressure at base centre in two-dimensional Oseen flow.
$v_i \equiv 0$, $\delta = \sqrt{(3/R)}$.

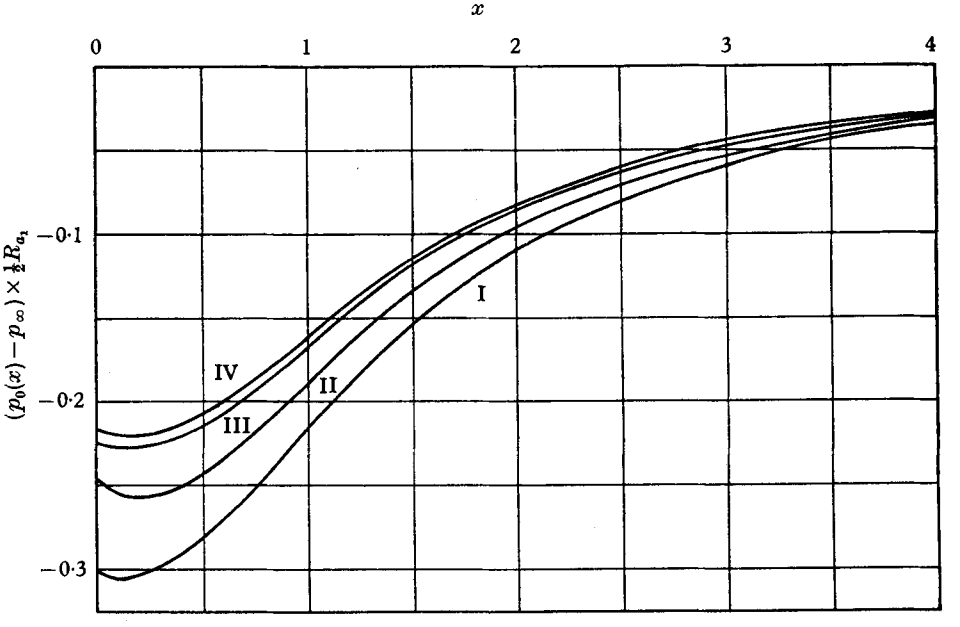

FIGURE 7. Pressure on x-axis in two-dimensional Oseen flow: influence of value of c.
$\delta = 1$, $v_i \equiv 0$. Curve I, $R = 0{\cdot}5$; II, $R = 1{\cdot}0$; III, $R = 2{\cdot}0$; IV, $R = 3{\cdot}0$.

we see that the velocity in the recirculating zone, although much higher than in Stokes flow, is at most of the order of a few percent of the free-stream velocity, even when this zone extends several base heights downstream.

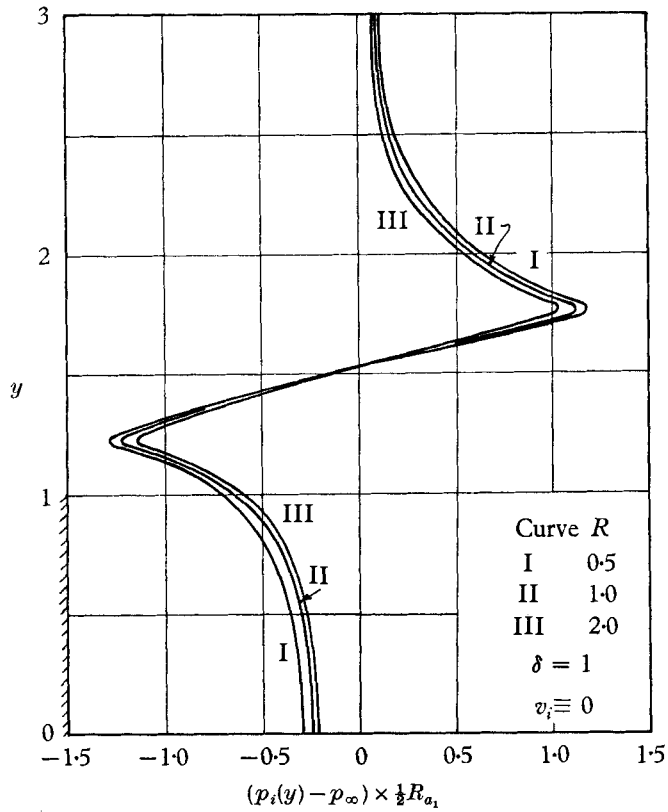

FIGURE 8. Pressure at $x = 0$ in two-dimensional Oseen flow: influence of value of c. $\delta = 1$, $v_i \equiv 0$. Curve I, $R = 0{\cdot}5$; II, $R = 1{\cdot}0$; III, $R = 2{\cdot}0$.

5.3. *Pressure*

Figure 4 shows the pressure on the x-axis, and figure 6 the pressure at the base centre ($x = 0$, $y = 0$) for various R and δ. The calculations give the quantity $(p_0(x) - p_\infty)/c$ so that the actual value of the pressure is not known until a value has been attributed to c; however, if we assume c to be constant as R and δ vary, the results still show the influence of the Reynolds number on the pressure.

We can compare the pressure at $R = 0$ (curve A, $\overline{p}_0(x) - \overline{p}_\infty$ of figure 7 of Part 1) with the pressure at $R = 3$ (curve II of figure 4), for practically identical boundary conditions, by using the relation $\overline{p}_0(x) - \overline{p}_\infty = 2R(p_0(x) - p_\infty)/c$; the pressure is found to be higher and more uniform at $R = 3$ than at $R = 0$.

The pressure at $x = 0$ (figure 8) was calculated only for $\delta = 1$, and various R, in order to study the influence of the value of c (see §5.4). Note the strong decrease of base pressure from the centre to the edge of the base, followed by a strong increase above the base and then a return to free-stream pressure. Since the separated-flow region behind the base is small in extent the flow must turn

sharply at the base. The pressure profile shown in figure 8, with its pronounced minimum and maximum, is necessary to cause the flow to make this sharp turn and then take up the recirculatory pattern characteristic of the separated-flow region.

5.4. *Influence of the value of c*

The influence of the value of c on the solution was studied in the case $\delta = 1$, for a fixed (unspecified) value of R_{a_1}; changes in R then come only from changes in c through the relation $R = \frac{1}{2}cR_{a_1}$.

The results for the velocity on the x-axis indicate changes with R of the order of magnitude of those shown in figure 3; we can conclude that the velocity, hence the position of the rear stagnation point, for fixed δ and R_{a_1}, are very sensitive to the value of c. This property could be used to determine an optimum value of c by comparison with experimental results, assuming that the calculations are made with an experimentally determined initial velocity profile.

The results for the pressure (figures 7 and 8) show a much smaller dependence on c. Since c is now the variable parameter, we must consider

$$(p-p_\infty)\,R/c = \tfrac{1}{2}(p-p_\infty)\,R_{a_1}$$

instead of $(p-p_\infty)/c$. Because of its large variations with y, the pressure at $x = 0$, $p_i(y)$, is less influenced, relatively speaking, than the pressure on the x-axis.

5.5. *The Stokes solution as a particular case of the Oseen solution*

It is clear that the method used to solve for the Oseen flow could be used in Stokes flow, the only difference being that we have $R = 0$, hence $K = \lambda$. This change can be made without difficulty in the expressions giving the vorticity and the pressure, equations (3.4), (3.18), (4.3) and (4.16). For the stream function, direct substitution is not possible. ψ_P, equations (3.10) or (4.9), of course, remains unchanged, but the integrand in equations (3.11) or (4.10) giving ψ_R, becomes of the form 0/0 if we let $R = 0$, $K = \lambda$. However, going back to Appendix I, we can solve for equation (A 4) again, where now $K = \lambda$, and we find $X_1 = (1/2\lambda)\,x\exp(-\lambda x)$.

Therefore, the results for ψ_R become, when $R = 0$, in two-dimensional flow

$$\psi_R = \tfrac{1}{2}x\int_0^\infty \exp(-\lambda x)\,[A(\lambda)\cos\lambda y + B(\lambda)\sin\lambda y]\,\frac{1}{\lambda}\,d\lambda, \tag{5.2a}$$

and in axisymmetric flow

$$\psi_R = \tfrac{1}{2}xy\int_0^\infty \exp(-\lambda x)\,J_1(\lambda y)\,A(\lambda)\,d\lambda. \tag{5.2b}$$

It is noteworthy that the decomposition used for the stream function in Oseen flow, $\psi = \psi_P + \psi_R$, becomes identical, when $R = 0$, to the one used in Stokes flow, equation (3.12) of Part 1, namely $\psi = V_1 - x(\partial V_1/\partial x + V_2)$; we thus have

$$\left.\begin{aligned}\psi_P &\equiv V_1,\\ \psi_R &\equiv -x\left(\frac{\partial V_1}{\partial x}+V_2\right),\end{aligned}\right\} \quad \text{when} \quad R = 0.$$

The relation between $\Omega_i(y)$, $v_i(y)$ and $u_i(y)$ takes the form, when $R = 0$, in two-dimensional symmetric flow, equation (2.32*b*),

$$B(\lambda) = -2\lambda\left[D(\lambda)+\frac{C(\lambda)}{\lambda}\right], \tag{5.3a}$$

and in axisymmetric flow, equation (4.19*b*),

$$A(\lambda) = -2\lambda\left[D(\lambda)+\frac{C(\lambda)}{\lambda}\right]. \tag{5.3b}$$

In the particular case $v_i(y) \equiv 0$, $D(\lambda) \equiv 0$, and we recover the result given in § 6.4

$$\Omega_i(y) = -2(du_i/dy).$$

6. Conclusions

The two-dimensional and axisymmetric base-flow problems at very low Reynolds numbers have been solved according to the Stokes and the Oseen approximations. The main conclusions which can be drawn from the study of the solutions and of numerical examples are the following:

(1) In the limit $R \to 0$, the flow is able to turn around the base edge and enter into the base region without creating an important separated-flow region. In Stokes flow ($R = 0$), there is no recirculating zone if $v_i(y) \leqslant 0$ or if $v_i(y) \equiv 0$ (for $y > 0$, symmetric flow); there is one if $v_i(y) \geqslant 0$ ($y > 0$), but it is of small extent, in the axial direction, as long as $v_i(y)$ remains small compared to $u_i(y)$.

As R increases, inertia effects tend to increase the length of the separated-flow region and, at the same time, to reduce the rate of increase of $u_0(x)$ with x; these effects seem to be very sensitive to the value of the Reynolds number.

(2) The base and near-wake regions are characterized by large velocity and pressure gradients; in particular, the base pressure varies strongly with y, decreasing from the centre to the edge of the base. As R increases, inertia effects tend to lessen the intensity of these gradients.

(3) A discontinuity in shear stress at $x = 0$ results in an infinite pressure at the point of discontinuity; as a consequence the initial velocity profile must be of the separation type, that is, we must have

$$du_i(y)/dy \to 0 \quad \text{as} \quad y \to 1+.$$

(4) There is a striking similarity between the two-dimensional and the axisymmetric cases in the method of solution and in the properties of these solutions. The only noticeable differences, observed in the numerical examples, and for identical boundary conditions, are quantitative; velocity and pressure gradients are appreciably higher, pressures are lower, and, in a general way, the departure from uniform flow is higher in axisymmetric flow than in two-dimensional flow.

As a final comment, we would like to point out that the solutions obtained here for Stokes and Oseen flows can be used in connexion with any prescribed velocity distribution in the plane $x = 0$; in particular, they could find applications in problems of jets issuing from the plane $x = 0$ into a fluid either at rest or having some non-zero velocity at infinity.

Appendix I

In this appendix we derive the solution for the rotational component of the stream-function ψ_R in Oseen flow.

Two-dimensional flow

ψ_R satisfies Poisson's equation

$$\nabla^2\psi_R = -\Omega(x,y), \tag{A 1}$$

with the boundary condition $$\psi_R(0,y) = 0. \tag{A 2}$$

Taking into account the form of Ω, equation (3.4), it is clear that ψ_R will be of the form

$$\psi_R = \int_0^\infty X_1(x;\lambda)\,[A(\lambda)\cos\lambda y + B(\lambda)\sin\lambda y]\,d\lambda. \tag{A 3}$$

Then equation (A 1) reduces to an ordinary differential equation for $X_1(x;\lambda)$ considered as a function of x only

$$X_1'' - \lambda^2 X_1 = -\exp(-Kx), \tag{A 4}$$

where a prime denotes differentiation with respect to x. The general solution of equation (A 4) is

$$X_1(x;\lambda) = -\frac{\exp(-Kx)}{K^2-\lambda^2} + \alpha_1\exp(\lambda x) + \alpha_2\exp(-\lambda x),$$

α_1 and α_2 being arbitrary constants.

We must take $\alpha_1 = 0$ so that $\psi_R \to 0$ as $x\to\infty$ and $\alpha_2 = 1/(K^2-\lambda^2)$ so that condition (A 2) be satisfied. Then

$$X_1(x;\lambda) = \frac{\exp(-Kx)-\exp(-\lambda x)}{\lambda^2-K^2} = \frac{\sqrt{(R^2+\lambda^2)}+R}{2R\lambda^2}\{\exp(-Kx)-\exp(-\lambda x)\}. \tag{A 5}$$

Hence ψ_R from equation (A 3)

$$\psi_R = \frac{1}{2R}\int_0^\infty [\sqrt{(R^2+\lambda^2)}+R][\exp(-Kx)-\exp(-\lambda x)] \times [A(\lambda)\cos\lambda y + B(\lambda)\sin\lambda y]\frac{1}{\lambda^2}\,d\lambda. \tag{A 6}$$

Axisymmetric flow

ψ_R satisfies

$$D^2\psi_R = -y\Omega(x,y), \quad \text{where} \quad D^2 \equiv \frac{\partial^2}{\partial x^2} + \frac{\partial^2}{\partial y^2} - \frac{1}{y}\frac{\partial}{\partial y}, \tag{A 7}$$

$$\psi_R(0,y) = 0, \tag{A 8}$$

$$\psi_R(x,0) = 0. \tag{A 9}$$

Ω is given by equation (4.3).

Writing

$$\psi_R = y\int_0^\infty X_2(x;\lambda)\,J_1(\lambda y)\,\lambda A(\lambda)\,d\lambda, \tag{A 10}$$

we find that $X_2(x;\lambda)$ must satisfy the same equation as X_1, equation (A 4), and the same boundary conditions, so that $X_2 \equiv X_1$. Use must be made of Bessel's equation. $J_1''(z) + (1/z)J_1'(z) + (1 - 1/z^2)J_1(z) = 0.$

Equation (A 10) then gives

$$\psi = \frac{1}{2R} y \int_0^\infty [\sqrt{(R^2+\lambda^2)} + R][\exp(-Kx) - \exp(-\lambda x)] J_1(\lambda y) \frac{A(\lambda)}{\lambda} d\lambda. \tag{A11}$$

Appendix II

We now indicate the main steps in the calculation of the numerical examples for Oseen flow.

First, we calculate $C(\lambda)$ according to equations (3.13) and (5.1); after several integrations by parts, we find

$$C(\lambda) = \frac{120}{\pi} \frac{1}{(\delta\lambda)^3} \left[(1 - 12/(\delta\lambda)^2)(\cos\{(\delta+1)\lambda\} - \cos\lambda) - \frac{6}{\delta\lambda}(\sin\{(\delta+1)\lambda\} + \sin\lambda) \right]. \tag{B 1}$$

Equation (B 1) is not suited for the calculation of $C(\lambda)$ at very small values of λ and we must use a series expansion

$$\frac{C(\lambda)}{\lambda} = \frac{60}{\pi} \sum_{n=0}^{\infty} C_{2n} \lambda^{2n}, \tag{B 2}$$

where

$$C_{2n} = (-1)^n \frac{2}{(2n+4)!} \frac{1}{\Delta^{2n+1}} \left[(\Delta+1)^{2n+4} - \Delta^{2n+4} - \frac{6}{2n+5}\{(\Delta+1)^{2n+5} + \Delta^{2n+5}\} + \frac{12}{(2n+5)(2n+6)}\{(\Delta+1)^{2n+6} - \Delta^{2n+6}\} \right], \tag{B 3}$$

and $\Delta = \delta^{-1}$.

By taking the first eight terms in the series, we found that $C(\lambda)/\lambda$ could be obtained with a quite sufficient accuracy up to $\lambda = 0{\cdot}4$. For $\lambda > 0{\cdot}4$ we used equation (B 1). $B(\lambda)$ can now be obtained from equation (3.23b) with $D(\lambda) \equiv 0$ (since $v_i \equiv 0$)

$$B(\lambda) = -[\sqrt{(R^2+\lambda^2)} + \lambda - R] \frac{C(\lambda)}{\lambda}. \tag{B 4}$$

Velocity on x-axis

Equation (3·17c) then gives

$$u_R(x,0) = \frac{-1}{2R} \int_0^\infty [\sqrt{(R^2+\lambda^2)} + R + \lambda][\exp(-Kx) - \exp(-\lambda x)] \frac{C(\lambda)}{\lambda} d\lambda. \tag{B 5}$$

$u_P(x,0)$ is given by equation (3.17b). $u_i(y)$ being a polynomial in y, we can integrate analytically, and the result is

$$u_P(x,0) = 1 - \frac{2}{\pi}\tan^{-1}\left(\frac{\delta+1}{x}\right) + \frac{2}{\pi}\delta^{-5}x \left[3\delta(\delta+2)(4x^2 + \tfrac{1}{2}\delta^2 - 4\delta - 4) + \{3x^4 - 5(\delta^2+6\delta+6)x^2 + 15(\delta+1)^2\} \ln\left\{\frac{x^2+(\delta+1)^2}{x^2+1}\right\} - \frac{1}{x}\{15(\delta+2)(x^2-2\delta-2)x^2 + 10\delta^2 + 15\delta + 6\} \times \left\{\tan^{-1}\left(\frac{\delta+1}{x}\right) - \tan^{-1}\left(\frac{1}{x}\right)\right\} \right]. \tag{B 6}$$

Pressure on x-axis

Equation (3.19) gives

$$\frac{p_0(x)-p_\infty}{c} = 1-u_0(x)-\frac{1}{2R}\int_0^\infty [\sqrt{(R^2+\lambda^2)}+R+\lambda]\exp(-Kx)\frac{C(\lambda)}{\lambda}d\lambda. \tag{B 7}$$

Pressure at $x = 0$

From equation (3.20) we deduce

$$\frac{p_i(y)-p_\infty}{c} = 1-u_i(y)-\frac{1}{2R}\int_0^\infty [\sqrt{(R^2+\lambda^2)}+R+\lambda]\cos\lambda y\frac{C(\lambda)}{\lambda}d\lambda. \tag{B 8}$$

Simpson's method of integration was used in successive intervals

$$(0,H),(H,2H)\ldots\{(n-1)H,nH\},$$

until the contribution from the last interval was found to be a negligible fraction (say 10^{-3}) of the total result.

Appendix III

In this appendix we consider a two-dimensional Oseen flow defined by an initial velocity profile $u_i(y)$ having a discontinuous slope at $y = 1$; we show that this leads to a logarithmically infinite pressure at this point.

The simplest profile having non-zero slope at $y = 1$ is a linear profile of the form

$$\left.\begin{aligned} u_i(y) &= \begin{cases} 0 & (0 \leqslant y \leqslant 1), \\ (y-1)/\delta & (1 \leqslant y \leqslant \delta+1), \\ 1 & (y \geqslant \delta+1), \end{cases} \\ u_i(-y) &= u_i(y) \quad \text{(symmetric flow)}. \end{aligned}\right\} \tag{C 1}$$

We also assume $v_i(y) \equiv 0$.

Therefore, from equation (3.13)

$$C(\lambda) = -\frac{2}{\pi\delta}\frac{1}{\lambda}[\cos\{(\delta+1)\lambda\}-\cos\lambda], \tag{C 2}$$

and the pressure at $x = 0$ can be obtained from equation (B 8) in Appendix II. Examination of equations (B 8) and (C 2) shows that the integrand in equation (B 8) presents no singularity for $\lambda \geqslant 0$. so that any possible divergence of the integral must come from the upper limit of integration, $\lambda \to \infty$.

For $\lambda \to \infty$, the integral behaves like

$$\int_{A>0}^\infty \frac{1}{\lambda}[\cos\{(y-1)\lambda\}-\cos\{(y-\delta-1)\lambda\}+\cos\{(y+1)\lambda\}-\cos\{(y+\delta+1)\lambda\}]d\lambda.$$

Let α stand for any of the following quantities:

$$|y-1|, \quad |y-\delta-1|, \quad |y+1|, \quad |y+\delta+1|.$$

We know that

$$\int_A^\infty \frac{\cos\alpha\lambda}{\lambda}d\lambda$$

is bounded as long as $\alpha \neq 0$. For $\alpha \to 0$, we can write

$$\int_A^\infty \frac{\cos \alpha\lambda}{\lambda} d\lambda = \int_{A\alpha}^\infty \frac{\cos t}{t} dt \sim \ln \alpha.$$

Thus we see that the pressure becomes logarithmically infinite at any of the points of discontinuity of du_i/dy.

We were not able to give a similar proof for axisymmetric Oseen flow; however, it is clear that such a proof, either in two-dimensional or in axisymmetric flow, is completely independent of the value of R.† Therefore, the above property concerning the pressure at $y = 1$, having been verified in axisymmetric Stokes flow ($R = 0$), holds also for $R \neq 0$ in axisymmetric Oseen flow.

This research has been supported by the Advanced Research Projects Agency and technically administered by the Fluid Dynamics Branch of the Office of Naval Research under Contract Nonr-222(45).

REFERENCES

BOWMAN, F. 1958 *Introduction to Bessel Functions.* New York: Dover Publications.

COURANT, R. & HILBERT, D. 1962 *Methods of Mathematical Physics,* vols. I and II. New York: Interscience.

LEWIS, J. A. & CARRIER, G. F. 1949 Some remarks on the flat plate boundary layer. *Quart. Appl. Math.* **7**, 228.

† Possible singularities in the integrand, and the behaviour of the integrand for $\lambda \to \infty$ are completely independent of R.